ASIAN JOURNAL OF PHARMACEUTICAL AND CLINICAL RESEARCH

INNOVARE ACADEMIC SCIENCES
Knowledge to Innovation

Vol 7, Issue 5, 2014

ISSN - 0974-2441

Research Article

MOLECULAR DOCKING STUDIES AND ABSORPTION, DISTRIBUTION, METABOLISM AND EXCRETION PREDICTION OF NOVEL ISATIN ANALOGS AS HUMAN IMMUNODEFICIENCY VIRUS-1-REVERSE TRANSCRIPTASE INHIBITORS WITH BROAD SPECTRUM CHEMOTHERAPEUTIC PROPERTIES

BIPLAB DEBNATH*, SWASTIKA GANGULY

Department of Pharmaceutical Sciences and Technology, Birla Institute of Technology, Mesra, Ranchi - 835 215, Jharkhand, India.
Email: biplab.d86@gmail.com

Received: 26 August 2014, Revised and Accepted: 13 September 2014

ABSTRACT

Molecular docking studies were performed on 100 newly designed isatin analogs using Glide v 5.0 on the active site of four different enzymes namely human immunodeficiency virus (HIV)-1 reverse transcriptase (RT) protein data bank (PDB ID 1RT2), glucosamine 6-phosphate (GlcN6P) (PDB ID 2VF5), *Mycobacterium tuberculosis*-CYP51 (PDB code 1EA1) and *Candida albicans* (CACYP51) (PDB code chimeric-1EA1) to study the binding mode of these analogs to study the binding mode of these analogs. Binding mode analysis of the compounds with the highest docking scores (−11.67, −7.31, −7.12 and −8.54) were carried out and compared with that of the co crystallized ligands TNK651, glucosamine (glucagon-like peptide) and fluconazole (TPF) in the active sites of 1RT2, 2VF5,1EA1, and chimeric 1EA1 respectively. Absorption, distribution, metabolism and excretion (ADME) properties of all the newly designed isatin analogs 1-100 was calculated by QikProp v 3.0. All the designed compounds were found to exhibit lead like properties from the calculated ADME properties. Results of these docking analyses can be well used for the design and development of novel isatin analogs possessing HIV-1-RT inhibitory activity with broad spectrum chemotherapeutic properties.

Keywords: Isatin analogs, Docking, Human immunodeficiency virus, Non-nucleoside reverse transcriptase inhibitors, Non-nucleoside inhibitory binding pocket, Lipinski's rule and absorption, distribution, metabolism and excretion.

INTRODUCTION

Acquired immune deficiency syndrome (AIDS) is one of the most vital challenges to public health care systems worldwide [1]. It is caused by human immunodeficiency virus (HIV), which belongs to the lent virus subfamily [2,3]. There are about 33 million people living with HIV/AIDS [4], whereas 25 million AIDS-related deaths have been reported in the last 25 years [5]. After so many years of its discovery, HIV is still a major health and socio-economic issue, specifically in developing countries [6].

During acute HIV infection, the virus directly infects CCR_5-expressing $CD4^+$Tcells, leading to their rapid depletion [7]. This result in a wide range of irreversible HIV-associated immunologic dysfunction or opportunistic infections like bacterial and fungal diseases, tuberculosis (TB), cancers, neurologic symptoms and wasting syndromes as well as it causes immunodeficiency [8]. Two main categories of HIV-reverse transcriptase (RT) inhibitors have been discovered to date. The first category of inhibitors is the nucleoside/nucleotide RT inhibitors (NRTIs), which bind to the enzymatic site of RT in a competitive manner with natural nucleotides and thereby terminates DNA synthesis after their incorporation into the growing DNA chain. The second groups of inhibitors are the non-NRTIs (NNRTIs), a group of structurally and chemically different compounds that non-competitively and selectively bind to the unique allosteric hydrophobic non-nucleoside inhibitory binding pocket (NNIBP) causing non-competitive inhibition of the viral polymerase [9].

TB is accountable for severe morbidity and mortality, mainly in developing countries where control interventions are remote, excessive and plagued by well-known drug resistance. It is caused by the intracellular pathogens *Mycobacterium* sp. It naturally affects the lungs (pulmonary TB), but can affect other organs as well as it can cause extra pulmonary TB. In 2010, there were an estimated 8.8 million new cases of *Mycobacterium tuberculosis* (MTB) and 1.5 million associated deaths, mostly occurring in developing countries. In India, one person dies of TB every minute [10,11] and India had the largest total incidence, with an estimated 2.0 million new cases [12]. Currently, TB is becoming a worldwide problem and it was declared since 1993 a global health emergency by the World Health Organization, the renaissance of TB became a serious world-wide problem during the period 1985-1992, particularly in people infected with the HIV. One of the major concerns is that it is the most common HIV-related opportunistic infection, thus treatment of the patients infected with both the diseases is a major challenge [13-15]. More than half a million people die from HIV-associated TB annually [16]. Lethal combination of TB and HIV infection for nearly the past three decades has posed a major threat to the international community's effort to achieve the health-related United Nations Millennium Development Goals for TB and HIV infection [17]. In addition to that, the emergence of drug-resistant strains of MTB has led to an enlarged pressure on present chemotherapy regimens.

Microbial infections have always been a growing problem in contemporary medicine, and the uses of antimicrobials are common across the world. Antimicrobials are, therefore, essential treatments, especially in the developing world where infectious diseases are a common cause of death. The rapid prevalence of the AIDS epidemic, as well as an increase in the use of immunosuppressant's, has also resulted in an abnormal increase in the incidence of systemic microbial infections. Antibiotics are among the most commonly used drugs, which are misused by physicians. The inevitable consequence of widespread and injudicious use of antibiotics has been the emergence of antibiotic-resistant pathogens, resulting in a serious threat to global public health [18]. This increase in resistance against the current day antibiotics demands to explore and synthesize a novel class of antimicrobial compounds effective against pathogenic microorganisms that have developed resistance to the antimicrobials used in the current regimen [19,20].

In recent years, due to the overzealous use of antibacterial antibiotics, the use of immunosuppressive agents, cytotoxins, irradiation and steroids, a new category of systemic mycoses has become prominent.

These are the opportunistic fungal infections. The patient, as a result of drug therapy, underlying disease, or medical manipulation, is deprived of the normal defenses conferred by microbial flora. This allows organisms of normally low inherent virulence to exploit the host. Oral candidiasis is common in poorly nourished persons, in patients on immunosuppressive drugs, and in persons with AIDS [21].

An ideal anti-HIV agent is one that not only suppresses HIV replication, but is also able to combat other opportunistic infections or a wide range of irreversible HIV-associated immunologic dysfunction. Though it is a known fact that NNRTI are selective in action [9], recently some NNRTIs like NAIMs analogs have shown inhibitory activities against HIV-2 and simian immunodeficiency virus [22]. On the basis of all these factors anti-HIV agents coupled with broad spectrum chemotherapeutic properties are vigorously searched for with persistence.

Isatin (1 H-indole-2, 3-dione), an endogenous compound identified in many organisms, shows a wide range of biological activities [23]. The isatin pharmacophore has attracted and still attracts much attention from medicinal chemists because of its structural resemblance to various moieties present in vitamins, proteins, and nucleic acids. From worldwide reported literature, the various isatin analogs are known to possess a range of biological properties, including antibacterial and antifungal [24-28], antiviral [29-31], anti-HIV [32,33], antiglycation [34], anticonvulsant, sedative-hypnotic [35,36], diuretic [37], anti-Alzheimer's activity [38] and anti-inflammatory [39] activities. Various isatin derivatives have been reported to possess cytotoxic activity [40-43]. Thus, isatin is a biologically validated starting point for the design and synthesis of chemical libraries directed at these targets [44].

In recent years, rational drug design has become prevalent widely in the pharmaceutical industry. This involves the use of computational methods which are simple, non-expensive and speed up the process of designing novel and potent molecules with desired biological activity. Docking is a rational approach to drug design that seeks to predict the structure and binding free energy of a ligand-receptor complex given only the structures of the free ligand and receptor [45]. The setup for a ligand docking approach requires the following components. A target protein structure with or without a bound ligand, the molecules of interest or a database containing existing or virtual compounds for the docking process, and a computational framework that allows the implementation of the desired docking and scoring procedures. Docking accuracy reflects an algorithm's ability to discover a conformation (pose) (http://poseview.zbh.uni-hamburg.de) and alignment of a ligand relative to a cognate protein that is close to that experimentally observed and to recognize the pose as correct. Scoring is the identification of the correct binding pose by its lowest energy value and the ranking of protein-ligand complexes according to their binding affinities [46]. Molecular docking is often used in virtual screening methods [47], whereby large virtual libraries of compounds are reduced in size to a manageable subset, which, if successful, includes molecules with high binding affinities to a target receptor.

MATERIALS AND METHODS

Computational methods by Glide 5.0

Docking study was performed for all the designed compounds 1-100 by Glide v 5.0 [48] installed in a single machine running on a 3.4 GHz pentium 4 processor with 1 GB RAM and 160 GB hard disk with Red Hat Linux Enterprise Version 5.0 as the operating system.

Protein structure preparation

The X-ray crystallographic structure of HIV-1-RT protein data bank (PDB entry code 1RT2) was obtained from Brookhaven PDB (RCSB) [49]. For docking studies, chain A was retained. All water molecules and chain B were removed from the complex, and the protein was minimized by the protein preparation wizard. Partial atomic charges were assigned according to the optimized potential for liquid simulations-all atom (OPLS-AA) force field. A radius of 10Å was selected for active site cavity during receptor grid generation.

Recent modeling studies have reported that glucosamine 6-phosphate (GlcN6P)-synthase may be acting as a unique target for inhibition by antimicrobials [50]. Considering this, the X-ray crystallographic structure of GlcN6P, was retrieved from Brookhaven (PDB entry code 2VF5). All water molecules and ligands were removed from the protein for docking studies, and the protein was minimized by the protein preparation wizard.

Similarly, the crystallographic structure of the enzyme MTB-CYP51 was also obtained from the Brookhaven (PDB entry code 1EA1). Missing atoms in the crystal structure were added, and the structure was optimized in a similar manner.

Although P-450$_{DM}$ enzymes have been purified from different sources [51,52], no experimental structural information on the active site of the target enzyme *Candida* P-450$_{DM}$ is available. A perusal of the literature showed that the high homology exists between the mycobacterium P-450$_{DM}$ and *Candida* P-450$_{DM}$. Based on the work of Rossello *et al*. [53], the chimeric enzyme for the *Candida albicans* (CACYP51) was constructed from that of *Mycobacterium* P-450$_{DM}$ MT CYP51 extracted from the (PDB entry code 1EA1). The residues that were arranged in a range of 7Åfrom fluconazole (TPF) were substituted with those of *Candida* P-450$_{DM}$. Only 12 substitutions were made by replacement of the residues Pro77, Phe78, Met79, Arg96, Met99, Leu100, Phe255, Ala256, His258, Ile322, Ile323 and Leu324 by Lys77, His78, Leu79, Leu96, Lys99, Phe100, Met255, Gly256, Gln258, His322, Ser323 and Ile324, which were thought to be necessary for the ligand-receptor interaction. The binding pocket for *Candida* P-450$_{DM}$ was obtained similarly as for 1EA1 and the protein prepared in a similar manner as given above.

Ligand structure preparation

All the compounds used in the docking study with glide were built within maestro by using build module of Schrodinger Inc. These structures were geometry optimized by means of the optimized potentials for liquid simulations-2005 (OPLS 2005) force field with the steepest tumble followed by reduced Newton conjugate gradient protocol. Partial atomic charges were computed using the OPLS-2005 force field.

Validation of docking protocol

The most suitable method of evaluating the precision of a docking procedure is to determine how closely the lowest energy pose predicted by the scoring function resembles an experimental binding mode as determined by X-ray crystallography. In the present study, extra precision (XP) glide docking procedure was validated by removing TNK651, glucosamine (glucagon-like peptide [GLP]) and TPF from the crystallographic structures of the proteins with PDB ID: 1RT2, 2VF5, 1EA1 respectively. We set up a very good concord between the localization of the inhibitors upon docking and from the crystal structures. The root mean square deviations (RMSDs) between the predicted conformation and the observed X-ray crystallographic conformation of compounds TNK651, GLP and flucanozole (TPF), equaled 2.445Å, 1.674Å and 2.744Å (>3Å) respectively. This indicates the reliability of the docking method in reproducing the experimentally observed binding mode for 1RT2, 2VF5 and 1EA1 and chimeric 1EA1.

Docking and scoring function

All the conformers from the Confgen-Ligprep output were docked in the NNIBP of 1RT2 and the active sites of 2VF5, 1EA1 and chimeric 1EA1. All default parameters were used for XP docking. Glide XP mode was employed for the current docking study. Best poses were chosen for energy minimization during docking, a distance-dependent dielectric constant of 2.0 and maximum number of minimization step of 100 was used. The docking simulations (ligand receptor interactions) are scored using the XP mode which is implemented in Glide v 5.0. Finally, the minimized poses were rescored using Schrodinger's proprietary glide score scoring function. In this docking method, the ligands are flexible, and receptor is rigid except that the protein active site, which has a

slight flexibility. To include receptor flexibility the ligands were docked into different grids generated for protein conformations [54,55].

Absorption, distribution, metabolism and excretion (ADME) prediction

ADME properties were calculated using QikProp v 3.0 tool of Schrodinger software [56]. QikProp provides ranges for comparing an exact molecule's properties with those of 95% of known drugs. QikProp also flags 30 types of reactive functional groups that may cause false positives in high throughput screening assays. It also evaluates the suitability of analogs based on Lipinski's rule of five [57], which is essential to ensure drug-like pharmacokinetic profile while using rational drug design. All the analogs were neutralized before being used by QikProp v3.0.

RESULTS AND DISCUSSION

Docking studies

In the present communication, a series of isatin analogs (Fig. 1) 1-100 (Table 1) was designed and have been used for molecular docking studies on the active sites of different proteins viz., 1RT2, 2VF5, 1EA1 and chimeric 1EA1 respectively by using Glide 5.0 [46]. The docking scores are depicted in Table 2.

Docking studies were performed using Glide v 5.0 in the active sites of four high resolution crystal structures of various enzymes in order to investigate the possible interactions between the designed isatin analogs and the active site of the different enzymes namely HIV-1 RT (PDB code 1RT2), GlcN6P (PDB code 2VF5), MTB-CYP51 (PDB code 1EA1) and *C. albicans* (CACYP51) (PDB code chimeric-1EA1) to study the binding mode of these analogs. The X-ray structure of the enzymes (PDB ID: 1RT2, 2VF5, 1EA1 and chimeric 1EA1) bound with TNK651, GLP and (TPF) was taken from the PDB.

The consistency of the docking results was first checked by comparing the best docking poses obtained for the co-crystallized inhibitor with its bound conformation. This was done by removing each ligand from their active site and subjecting again to redocking into the binding pocket in the conformation found in the crystal structure. Thus, a RMSD of 1.737Å, 1.005Å, 2.744Å, and 2.931A° for proteins PDB ID: 1RT2, 2VF5 and 1EA1 cocrystalized with TNK651, GLP and (TPF) respectively was found signifying that the docking procedure could be relied to predict the binding mode of our compounds.

To illustrate the binding mode of the isatin analogs in the NNIBP of 1RT2 and in the active sites of 2VF5, 1EA1 and chimeric 1EA1, the docking pose of active compounds 47, 88, 13 and 38 (Glide XP score −11.67, −7.31, −7.12 and −8.54), respectively have been discussed as follows.

The three dimensional docked pose of TNK651 in the active site of 1RT2 has been depicted in Fig. 2a and the residues involved in inter atomic contact has been shown in the schematic 2D representation as in Fig. 2b.

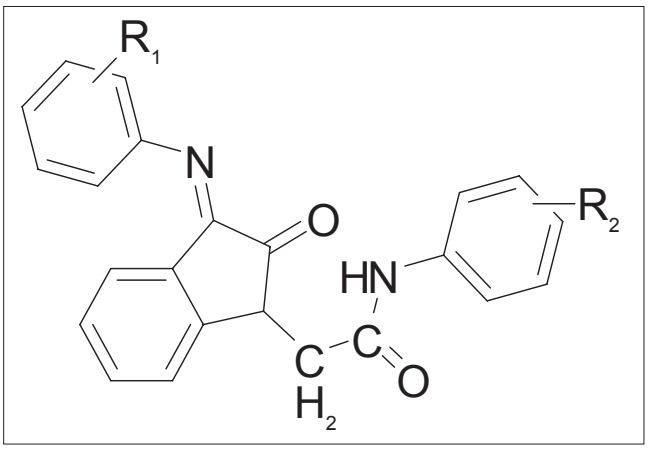

Fig. 1: Structure of Isatin analogs

The binding mode of compound 47 in the active site of 1RT2 has been represented in its three dimensional mode in Fig. 3a while the schematic 2D dimensional representation has been shown in Fig. 3b. The phenyl ring in the isatin moiety is favorably interacting with Tyr 188, a key

Table 1: Structures of newly designed isatin analogs 1-100

Compound code	R_1	R_2	Compound code	R_1	R_2
1	-H	-H	51	-3-CH_3	-H
2	-H	-2-Cl	52	-3-CH_3	-2-Cl
3	-H	-3-Cl	53	-3-CH_3	-3-Cl
4	-H	-4-Cl	54	-3-CH_3	-4-Cl
5	-H	-2-CH_3	55	-3-CH_3	-2-CH_3
6	-H	-4-CH_3	56	-3-CH_3	-4-CH_3
7	-H	3-OCH_3	57	-3-CH_3	3-OCH_3
8	-H	4-OCH_3	58	3-CH_3	4-OCH_3
9	-H	4-Br	59	3-CH_3	4-Br
10	-H	-3,4-CH_3	60	3-CH_3	-3,4-CH_3
11	-2-Cl	-H	61	3-OCH_3	-H
12	-2-Cl	-2-Cl	62	3-OCH_3	-2-Cl
13	-2-Cl	-3-Cl	63	3-OCH_3	-3-Cl
14	-2-Cl	-4-Cl	64	3-OCH_3	-4-Cl
15	-2-Cl	-2-CH_3	65	3-OCH_3	-2-CH_3
16	-2-Cl	-4-CH_3	66	3-OCH_3	-4-CH_3
17	-2-Cl	3-OCH_3	67	3-OCH_3	3-OCH_3
18	-2-Cl	4-OCH_3	68	3-OCH_3	4-OCH_3
19	-2-Cl	4-Br	69	3-OCH_3	4-Br
20	-2-Cl	-3,4-CH_3	70	3-OCH_3	-3,4-CH_3
21	-3-Cl	-H	71	4-OCH_3	-H
22	-3-Cl	-2-Cl	72	4-OCH_3	-2-Cl
23	-3-Cl	-3-Cl	73	4-OCH_3	-3-Cl
24	-3-Cl	-4-Cl	74	4-OCH_3	-4-Cl
25	-3-Cl	-2-CH_3	75	4-OCH_3	-2-CH_3
26	-3-Cl	-4-CH_3	76	4-OCH_3	-4-CH_3
27	-3-Cl	3-OCH_3	77	4-OCH_3	3-OCH_3
28	-3-Cl	4-OCH_3	78	4-OCH_3	4-OCH_3
29	-3-Cl	4-Br	79	4-OCH_3	4-Br
30	-3-Cl	-3,4-CH_3	80	4-OCH_3	-3,4-CH_3
31	-4-Cl	-H	81	-4-Br	-H
32	-4-Cl	-2-Cl	82	-4-Br	-2-Cl
33	-4-Cl	-3-Cl	83	-4-Br	-3-Cl
34	-4-Cl	-4-Cl	84	-4-Br	-4-Cl
35	-4-Cl	-2-CH_3	85	-4-Br	-2-CH_3
36	-4-Cl	-4-CH_3	86	-4-Br	-4-CH_3
37	-4-Cl	3-OCH_3	87	-4-Br	3-OCH_3
38	-4-Cl	4-OCH_3	88	-4-Br	4-OCH_3
39	-4-Cl	4-Br	89	-4-Br	4-Br
40	-4-Cl	-3,4-CH_3	90	-4-Br	-3,4-CH_3
41	-2-CH_3	-H	91	-3,4-CH_3	-H
42	-2-CH_3	-2-Cl	92	-3,4-CH_3	-2-Cl
43	-2-CH_3	-3-Cl	93	-3,4-CH_3	-3-Cl
44	-2-CH_3	-4-Cl	94	-3,4-CH_3	-4-Cl
45	-2-CH_3	-2-CH_3	95	-3,4-CH_3	-2-CH_3
46	-2-CH_3	-4-CH_3	96	-3,4-CH_3	-4-CH_3
47	-2-CH_3	3-OCH_3	97	-3,4-CH_3	3-OCH_3
48	-2-CH_3	4-OCH_3	98	-3,4-CH_3	4-OCH_3
49	-2-CH_3	4-Br	99	-3,4-CH_3	4-Br
50	-2-CH_3	-3,4-CH_3	100	-3,4-CH_3	-3,4-CH_3

Table 2: Results of molecular docking studies of compounds 1-100 in the active sites of proteins (PDB ID1M17, 2J5F, 2ITW, 2ITX and 2ITY) performed using extra precision mode of Glide

Compound	1RT2 (G score)	1EA1 (G score)	Chimeric 1EA1 (G score)	2VF5 (G score)
Reference	−13.21	−5.735	−5.735	−6.56
1	−10.55	−6.1	−7.67	−6.47
2	−7.85	−3.02	−6.35	−0.95
3	−10.31	−5.33	−8.24	−5.72
4	−10.07	−4.65	−6.88	−4.82
5	−10.39	−5.06	−7.64	−5.33
6	−9.11	−3.62	−7.15	−6.65
7	−7.32	−5.48	−7.08	−5.86
8	−10.53	−6.3	−5.93	−2.04
9	−9.13	−5.06	−7.02	−5.25
10	−10.12	−6.08	−5.62	−6.44
11	−10.92	−5.97	−7.38	−6.36
12	−9.12	−6.27	−6.84	−6.62
13	−10.7	−7.12	−7.96	−6.8
14	−10.49	−6.91	−7.76	−7.15
15	−9.17	−5.79	−7.04	−6.2
16	−10.56	−6.81	−6.13	−7.1
17	−11.14	−6.57	−7.72	−6.82
18	−10.26	−6.78	−6.96	−7.05
19	−10.9	−3.3	−6.31	−1.84
20	−9.63	−6.61	−8.11	−6.86
21	−10.44	−5.76	−8.11	6.16
22	−10.3	−5.56	−7.66	−5.96
23	−10.54	−5.75	−7.35	−6.15
24	−7.71	−5.55	−6.97	−5.92
25	−10.61	−5.56	−7.6	−5.95
26	−10.5	−6.3	−7.83	−6.63
27	−10.58	−5.53	−7.44	−5.73
28	−10.46	−5.76	−6.73	−6.16
29	−10.59	−6.92	−6.54	−7.16
30	−7.63	−5.2	−7.28	−5.56
31	−9.11	−6.45	−7.48	−6.77
32	−9.93	−6.45	−7.58	−6.73
33	−10.15	−6.76	−7.95	−7.02
34	−9.47	−5.76	−7.14	−7.08
35	−9.26	−6.44	−7.69	−6.74
36	−9.24	−6.8	−7.26	−7.08
37	−7.13	−6.77	−8.21	−7.04
38	−9.28	−6.93	−8.54	−7.16
39	−7.36	−6.84	−6.9	−7.11
40	−7.48	−6.9	−7.3	−7.14
41	−10.84	−6.05	−8.17	−6.42
42	−9.32	−6.25	−7.67	−6.6
43	−9.77	−6.2	−7.19	−6.56
44	−10.36	−5.8	−6.35	−6.2
45	−9.2	−6.14	−8.43	−6.5
46	−11.27	−6.09	−6.68	−6.44
47	−11.67	−5.21	−8.27	−5.56
48	−10.7	−6.76	−8.45	−7.02
49	−10.34	−5.84	−7.24	−6.23
50	−9.68	−5.7	−7.41	−6.08
51	−9.14	−6.42	−7.74	−6.72
52	−7.25	−6.2	−7.42	−6.57
53	−9.49	−6.62	−7.94	−6.87
54	−9.36	−5.75	−7.63	−6.15
55	−9.38	−6.12	−7.66	−6.49
56	−9.16	−5.94	−7.61	−6.34
57	−10.3	−6.42	−7.78	−6.72
58	−9.61	−6.84	−7.92	−7.11
59	−10.66	−5.67	−7.35	−6.05
60	−9.32	−6.48	−7.33	−6.79
61	−11.35	−5.73	−7.9	−6.13
62	−10.48	−5.07	−7.17	−5.36
63	−10.57	−5.85	−8.13	−6.25
64	−11.3	−5.72	−6.85	−6.12
65	−10.23	−6.41	−8.08	−6.72
66	−7.86	−6.13	−7.39	−6.5
67	−9.38	−6.23	−6.74	−6.6
68	−10.93	−5.64	−7.14	−6.03
69	−11.01	−5.25	−7.18	−5.65
70	−9.93	−6.79	−7.57	−7.07
71	−9.13	−6.72	−7.66	−6.96
72	−6.97	−6.54	−7.08	−6.8
73	−9.89	−6.61	−7.31	−6.86
74	−9.92	−7.04	−7.46	−7.22
75	−8.24	−6.45	−7.55	−6.77
76	−10.46	−6.8	−7.35	−7.07
77	−9.72	−6.93	−7.93	−7.16
78	−9.2	−7	−7.66	−7.18
79	−8.72	−4.83	−7.14	−4.97
80	−8.04	−6.73	−7.38	−6.97
81	−10.12	−6.36	−7.33	−6.69
82	−11.27	−6.31	−6.94	−6.66
83	−10.22	−6.67	−7.67	−6.93
84	−10.42	−6.85	−7.44	−7.12
85	−8.75	−6.23	−7.38	−6.6
86	−8.1	−6.64	−7.11	−6.9
87	−7.45	−6.71	−6.76	−6.95
88	−7.27	−6.99	−7.47	−7.31
89	−7.19	−4.68	−7.63	−4.46
90	−9.69	−6.82	−6.25	−7.11
91	−9.57	−6.47	−7.83	−6.79
92	−9.41	−5.78	−7.52	−6.19
93	−10.28	−6.53	−7.41	−7.28
94	−10.91	−6.71	−8.05	−6.95
95	−10.01	−6.4	−7.64	−6.72
96	−11.07	−7.11	−7.24	−7.27
97	−9.9	−6.75	−7.85	−7.01
98	−9.84	−7.11	−6.77	−7.19
99	−9	−6.82	−7.47	−7.11
100	−9.84	−6.89	−7.69	−7.14

(*Contd...*)

Table 2: (*Continued*)

PDB: Protein data bank

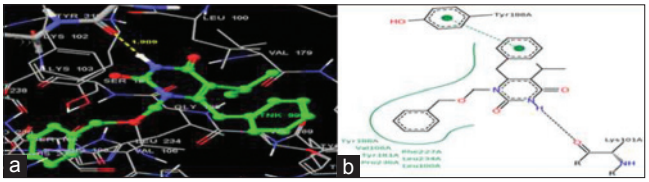

Fig. 2: (a) Redocked conformer of TNK651 in the active site of the protein human immunodeficiency virus-1-reverse transcriptase (RT) (protein data bank ID 1RT2), (b) 2D representation of the ligand TNK651

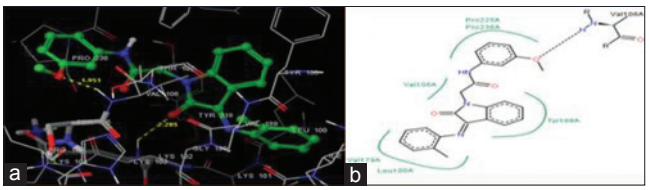

Fig. 3: (a) Molecular model of most active molecule in the compound 47 in the non-nucleoside inhibitory binding pocket of human immunodeficiency virus-1-reverse transcriptase (protein data bank code 1RT2). (Glide XP Score-11.67). Active site amino acid residues are represented as tubes, while the inhibitor is shown as ball and stick model with the atoms colored as carbon: green, hydrogen: cyan, nitrogen: blue, oxygen: red. Hydrogen bond interaction is represented by pink dotted lines, (b) Schematic (2D) representation of interactions of compound 47 in the binding pocket of the protein

residue in the NNIBP. The phenyl ring substituted with a methyl group at ortho position attached to the third position of the isatin moiety is embedded in the hydrophobic pocket formed by the side chains of Val 179 and Leu 108 while the other phenyl ring substituted with methoxy group at para position separated from the isatin moiety by the linker group CH_2-CO-NH occupied the other hydrophobic pocket formed by the side chains of Pro 225, Pro 236 and Val 106. Compound 47 shows two H-bond interactions, one between the methoxy group substituted at the meta position of the phenyl ring with the NH group present in the Val 106 residue ($OCH_{3\ phenyl\ ring}$-$NH_{Val\ 106}$=1.951Å) and the second one being between the C=O group present in the isatin moiety linkage with NH group present in Lys 101 residue (CO isatin ring-NH-Lys 101=2.285Å) These interactions may be responsible for the binding affinity of the molecule as indicated by the docking score −11.67. However, this score was found to be lesser than the docking score −13.21 of the reference ligand TNK 651.

The next protein (PDB ID 2VF5) co-crystallized with the ligand GLP also shows seven H-bond interactions (GLP phosphate metal with oxygen contains 4-H bonds and GLP basic ring contains 3-H bonds) present between the receptor residues and side chains of Ala 602, Val 399, Thr 352, Thr 302, Ser 349, Ser 303, Ser 347, Ala 400, Cys 300, Lys 603, Gly 301 and Gln 348 respectively (Fig. 4a and b). Among all the novel designed isatin analogs, compound 88 with the highest docking score in the active site of 2VF5 is visualized in its three dimensional mode in Fig. 5a and the residues involved in inter-atomic contact has been shown in Fig. 5b. Analysis of the docking pose of compound 88 in the active site of 2VF5 showed that the phenyl ring in the isatin moiety is favorably interacting with the residue Gly 301. The phenyl ring substituted with methyl group at *para* position attached to the third position of the isatin moiety interacts with the side chains of Thr 352, Thr 302, Ser 349, Ser 303, Ser 347, Ala 400 which shows similarity to the standard GLP in the active site of 2VF5 as mentioned above. The other phenyl ring substituted with a para bromo group separated from the isatin moiety by the linker group CH_2-CO-NH interacts with the side chains of Cys 300, Lys 603, Gln 348 and Thr 302. The compound also shows four H-bond interactions, first one between the C=O group of the -CH_2CONH and the NH group present in residue Thr 302 ($CO_{CH2CONH}$-NH_{Thr302}=1.935Å), the second one between the C=N group present at the 3rd position of the isatin moiety with NH group present in Ala 602 residue ($NH_{isatin\ ring}$-NH_{Ala602}=2.358Å), the third and the fourth one being between the methoxy group substituted at the para position of the phenyl ring with the OH group present in the Thr 352 and Ser 347 residues ($OCH_{3\ phenyl\ ring}$-OH_{Thr352} = 1.932Å) and ($OCH_{3\ phenyl\ ring}$-OH_{Ser347} =2.024 Å), respectively. These hydrogen bond interactions may be responsible for the high docking score of compound 88 (−7.31) which was found to be higher than that of the co-crystallized ligand GLP (6.56).

The 1EA1 X-ray crystal structure co-crystallized with the ligand flucanazole (TPF) is depicted in Fig. 6a and b. The docking pose of compound 13 in the active site of 1EA1 has been represented in its three-dimensional mode in Fig. 7a while the schematic 2D dimensional representation has been shown in Fig. 7b. The docking pose analysis revealed that the phenyl ring in the isatin moiety is oriented to interact with the side chains of Phe 78 and Thr 260. The phenyl ring substituted with chloro group at *ortho* position attached to the third position of the isatin moiety is interacts with the chain of Leu 321 while the other phenyl ring substituted with chloro group at *meta* position separated from the isatin moiety by the linker spacer CH_2-CO-NH interacts with the side chain of Ala 256 and Arg 326. The compound also shows one H-bond interaction, between C=O group of isatin and NH group present in residue Arg 326 ($C{=}O_{\ isatin\ ring}$ ___$NH_{\ Arg\ 326}$= 1.907Å). These interactions increase the binding affinity of the molecule as indicated by the docking score of the compound 13 as −7.12 comparable and more than the dock score −5.735 of the reference ligand TPF.

In case of the next protein (PDB ID chimeric 1EA1), for comparison purposes TPF was docked into the active site of chimeric 1EA1 (Fig. 8a and b) and the docking score obtained was (−5.735). In this case, compound 38, showed the highest docking score (−8.54) in the active site of chimeric 1EA1 [25]. In fact, the dock score was higher than that of the co-crystallized ligand TPF (−5.735). A three dimensional representation of the docked pose of compound 38 has been shown in Fig. 9a and the residues involved in inter-atomic contact has been shown in Fig. 9b. The docking pose study of compound 38 revealed that the isatin scaffold is oriented in the binding site likewise as in the case of the co crystallized ligand TPF in the active site of chimeric 1EA1. The

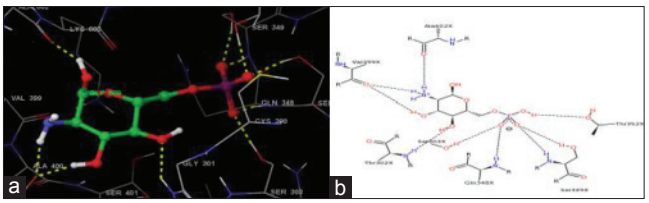

Fig. 4: (a) Redocked conformer of GLP in the active site of the protein glucosamine 6-phosphate (protein data bank ID 2VF5), (b) 2D representation of the ligand glucagon-like peptide

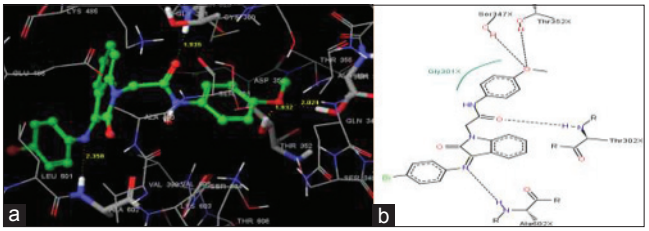

Fig. 5: (a) Molecular model of most active molecule in the compound 88 in the protein glucosamine 6-phosphate (protein data bank ID 2VF5)). (Glide XP Score-7.31). Active site amino acid residues are represented as tubes, while the inhibitor is shown as ball and stick model with the atoms colored as carbon: green, hydrogen: cyan, nitrogen: blue, oxygen: red. Hydrogen bond interaction is represented by pink dotted lines, (b) Schematic (2D) representation of interactions of compound 88 in the binding pocket of the protein

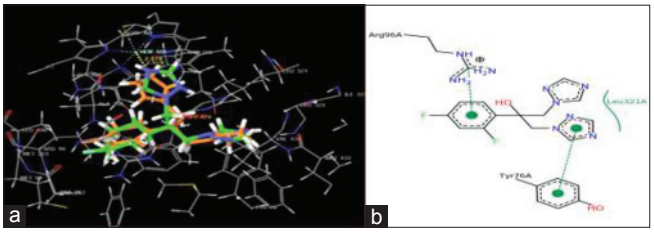

Fig. 6: (a) Redocked conformer of TPF in the active site of the protein *Mycobacterium tuberculosis*-CYP51 (protein data bank ID 1EA1), 6(b) D representation of the ligand TPF

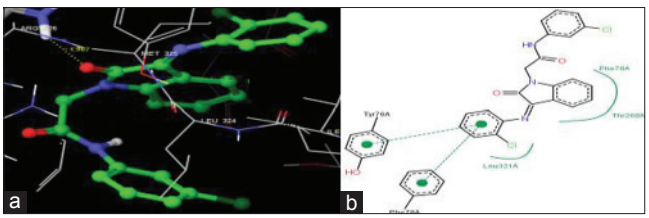

Fig.7: (a) Molecular model of most active molecule in the compound 13 in the protein *Mycobacterium tuberculosis*-CYP51 (protein data bank ID 1EA1) (Glide XP Score-7.12). Active site amino acid residues are represented as tubes, while the inhibitor is shown as ball and stick model with the atoms colored as carbon: green, hydrogen: cyan, nitrogen: blue, oxygen: red. Hydrogen bond interaction is represented by pink dotted lines, (b) Schematic (2D) representation of interactions of compound 13 in the binding pocket of the protein

phenyl ring in the isatin moiety is embedded in the hydrophobic pocket formed by the Phe 83, Phe 255 and Ala 256. The phenyl ring substituted with chloro group at ortho position attached to the third position of the isatin moiety interacts with the side chains of Arg 96 while the other phenyl ring substituted with methoxy group at para position separated from the isatin moiety by the linker spacer CH_2-CO-NH favorably interacts with the side chain of Val 395, Thr 260 and Tyr 76. The compound also shows one H-bond interaction, between the methoxy group substituted at the para position of the phenyl ring with the NH group present in the Val 395 residue ($OCH_{3\ phenyl\ ring}$-$NH_{\ Val\ 395}$= 2.189Å). These interactions and hydrogen bonding may be responsible for increasing the binding affinity of the molecule significantly as indicated by a very high docking score of the compound 38 (−8.54) comparable and more than the dock score −5.735 of the reference ligand TPF.

ADME properties

We have analyzed 100 physically descriptors and pharmaceutically significant properties of isatin analogs using QikProp v3.0 tool of Schrodinger software, among which major descriptors reported here are required for predicting the drug-like properties of molecules. These properties are:

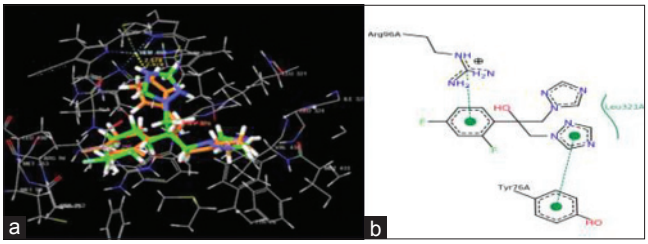

Fig. 8: (a) Redocked conformer of TPF in the active site of the protein *Mycobacterium tuberculosis*-CYP51 (protein data bank ID chimeric 1EA1), (b) 2D representation of the ligand TPF

1. Molecular weight (mol MW) (150-650)
2. Octanol/water partition coefficient (Log Po/w) (−2-6.5)
3. Aqueous solubility (QPlogS) (−6.5-0.5)
4. Apparent Madin–Darby canine kidney (MDCK) cell permeability (QPPMDCK) (<25 poor, >500 great)
5. Brain/blood partition coefficient (QPlogBB) (−3.0-1.2)
6. Percent human oral absorption (≥80% is high, ≤25% is poor).

All the structures showed significant values for the properties analyze and exhibited drug-like characteristics based on Lipinski's rule of 5. The ADME values of newly designed compounds 1-100 are given in Table 3. The first three properties are based on Lipinski rule of five, molecular weight (mol.MW)<650, partition coefficient between octanol and water (logPo/w) between −2 and 6.5 and solubility (QPlogS)>−7.

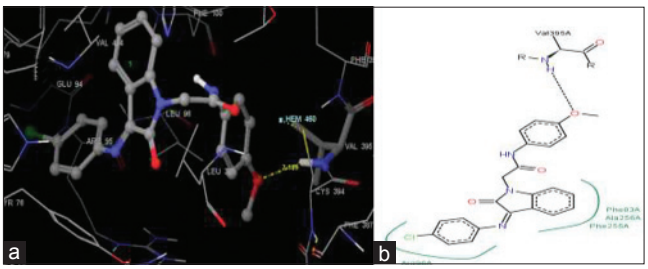

Fig. 9: (a) Molecular model of most active molecule in the compound 38 in the protein *Candida* P-450DM (protein data bank ID chimeric 1EA1) (Glide XP Score-8.54). Active site amino acid residues are represented as tubes, while the inhibitor is shown as ball and stick model with the atoms colored as carbon: Green, hydrogen: Cyan, nitrogen: Blue, oxygen: Red. Hydrogen bond interaction is represented by pink dotted lines, (b) Schematic (2D) representation of interactions of compound 38 in the binding pocket of the protein

Table 3: Prediction of ADME properties of newly designed isatin analogs using QikProp

Compound code	Mol. Wt.	Log Po/w	Log S	Log BB	PMDCK	Human oral absorption (%)	Rule of five
1	355.395	3.665	−5.066	−0.782	537.838	100	0
2	389.84	4.181	−5.382	−0.433	1529.7	100	0
3	389.84	4.451	−5.995	−0.378	2403	100	0
4	389.84	4.451	−5.992	−0.377	2410.1	100	0
5	369.422	4.115	−5.288	−0.498	1008.6	100	0
6	369.422	4.268	−5.827	−0.558	976.111	100	0
7	385.421	4.047	−5.377	−0.588	1016	100	0
8	385.421	4.036	−5.416	−0.611	976.068	100	0
9	434.291	3.388	−4.758	−1.1	276.456	100	0
10	383.449	4.535	−6.238	−0.0569	973.002	100	0
11	389.84	4.107	−5.607	0.603	1233.9	100	0
12	424.285	4.327	−5.73	−0.494	1930.2	100	0
13	424.285	4.595	−6.349	−0.451	3028.9	100	0
14	424.285	4.597	−6.341	−0.449	3045.7	100	0
15	403.867	4.183	−5.637	−0.56	1272.8	100	0
16	403.867	4.414	−6.178	−0.632	1230.6	100	0
17	419.866	4.565	−5.784	−0.685	1230.9	100	0
18	419.866	4.189	−5.77	−0.684	1230.2	100	0
19	417.894	4.155	−6.594	−0.647	1226.6	100	0
20	468.736	3.47	−5.663	−1.529	179.204	100	0
21	389.84	4.156	−5.8	−0.629	1326.9	100	0
22	424.285	4.375	−5.921	−0.518	2076.2	100	0
23	424.285	4.647	−6.538	−0.476	3266.1	100	0
24	424.285	4.647	−6.535	−0.475	3275.8	100	0
25	403.86	4.236	−5.827	−0.584	1368.3	100	0
26	403.867	4.122	−6.37	−0.658	1326.8	100	0
27	419.866	3.889	−5.959	−0.691	1381.1	100	0
28	419.866	4.784	−5.955	−0.709	1325.6	100	0
29	468.736	4.616	−6.394	−0.613	1369.6	100	0
30	417.894	4.731	−6.783	−0.672	1322.4	100	0
31	389.84	4.646	−5.799	−0.628	1327.9	100	0
32	424.285	4.648	−6.353	−0.405	3500.8	100	0

(*Contd...*)

Table 3: (*Continued*)

Compound code	Mol. Wt.	Log Po/w	Log S	Log BB	PMDCK	Human oral absorption (%)	Rule of five
33	424.285	3.581	−6.538	−0.476	3274.1	100	0
34	424.285	4.632	−6.534	−0.475	3277.9	100	0
35	403.867	3.558	−6.531	−0.443	2317.8	100	0
36	403.867	4.552	−6.365	−0.657	1327.9	100	0
37	419.866	4.248	−5.969	−0.696	1382.3	100	0
38	419.866	4.231	−5.956	−0.709	1327.4	100	0
39	468.736	4.787	−6.76	−0.592	1552.2	100	0
40	417.894	4.731	−6.782	−0.672	1323.2	100	0
41	369.422	3.959	−6.173	−0.651	1547.9	100	0
42	403.867	4.436	−5.975	−0.507	1618.8	100	0
43	403.867	4.451	−6.161	−0.575	1507.8	100	0
44	403.867	4.45	−6.174	−0.579	174.529	100	0
45	383.449	4.114	−5.45	−0.686	634.361	100	0
46	383.449	4.265	−5.988	−0.756	614.087	100	0
47	399.448	4.053	−5.584	−0.791	639.231	100	0
48	399.448	4.034	−5.579	−0.609	613.9	100	0
49	448.318	3.551	−5.629	−0.541	1544.5	100	0
50	397.476	3.148	−5.658	−0.553	1550.5	100	0
51	369.422	3.97	−5.629	−0.811	537.65	100	0
52	403.867	4.19	−5.751	−0.701	841.189	100	0
53	403.867	4.461	−6.367	−0.659	1322.9	100	0
54	403.867	4.461	−6.364	−0.657	1327	100	0
55	383.449	4.124	−5.658	−0.766	554.74	100	0
56	383.449	4.276	−6.196	−0.84	537.619	100	0
57	399.448	4.056	−5.746	−0.867	559.555	100	0
58	399.448	4.045	−5.785	−0.891	537.422	100	0
59	448.318	4.432	−6.227	−0.795	555.302	100	0
60	397.476	4.546	−6.414	−0.855	535.698	100	0
61	385.421	3.744	−5.232	−0.863	537.865	100	0
62	419.866	3.964	−5.355	−0.753	841.508	100	0
63	419.866	4.234	−5.967	−0.711	1323.7	100	0
64	419.866	4.234	−5.965	−0.709	1327.5	100	0
65	399.448	3.899	−5.261	−0.819	554.993	100	0
66	399.488	4.049	−5.795	−0.892	537.842	100	0
67	430.419	3.835	−5.386	−0.925	559.748	100	0
68	430.419	3.817	−5.384	−0.943	537.664	100	0
69	464.317	4.373	−6.189	−0.827	628.756	100	0
70	413.475	4.317	−6.811	−0.831	627.953	100	0
71	385.421	3.747	−5.248	−0.865	537.6	100	0
72	419.866	3.967	−5.371	−0.756	841.247	100	0
73	419.866	4.238	−5.985	−0.713	1325.4	100	0
74	419.866	4.237	−5.981	−0.712	1327	100	0
75	399.488	4.071	−5.639	−0.801	629.366	100	0
76	399.488	4.052	−5.811	−0.894	537.621	100	0
77	415.488	3.825	−5.413	−0.947	537.631	100	0
78	415.488	3.82	−5.4	−0.946	537.329	100	0
79	464.317	4.27	−5.841	−0.85	555.348	100	0
80	413.475	4.319	−6.224	−0.909	535.773	100	0
81	434.291	4.045	−5.785	−0.891	537.422	100	0
82	468.736	4.432	−6.227	−0.795	555.302	100	0
83	468.736	4.546	−6.414	−0.855	535.698	100	0
84	468.736	3.744	−5.232	−0.863	537.865	100	0
85	448.318	3.964	−5.355	−0.753	841.508	100	0
86	448.318	4.234	−5.967	−0.711	1323.7	100	0
87	464.317	4.234	−5.965	−0.709	1327.5	100	0
88	464.317	3.899	−5.261	−0.819	554.993	100	0
89	513.187	4.049	−5.795	−0.892	537.842	96.767	1
90	462.345	4.045	−5.785	−0.891	537.422	100	0
91	383.449	4.265	−6.004	−0.761	610.735	100	0
92	417.849	4.492	−6.138	−0.653	960.259	100	0
93	417.849	4.757	−6.745	−0.608	1503.2	100	0
94	417.849	4.757	−6.742	−0.607	1057.7	100	0
95	397.476	4.419	−6.013	−0.714	634.239	100	0
96	397.476	4.573	−6.574	−0.788	610.752	100	0
97	413.475	4.35	−6.125	−0.817	635.625	100	0
98	413.475	4.348	−6.174	−0.84	613.603	100	0
99	462.345	4.733	−6.608	−0.744	633.935	100	0
100	411.502	4.727	−6.583	−0.741	635.046	100	0
TNK651	366.459	3.363	−6.794	−2.016	69.627	86.235	0
1EA1	259.15	4.573	−6.183	−1.741	69.627	100	0
2VF5	306.27	4.286	−6.940	−0.941	69.627	100	0

ADME: Absorption, distribution, metabolism and excretion, PMDCK: Permeability Maden–Darby canine kidney

Brain/blood partition coefficient (QPlogBB) parameter indicated about the ability of the drug to pass through the blood-brain barrier which is mandatory for inhibition. The QPPMDCK predicted apparent MDCK cell permeability in nm/s. MDCK cells are considered to be a good mimic for the blood-brain barrier and higher the value of QPPMDCK, higher the cell permeability. All designed compounds showed ADME properties in acceptable range.

CONCLUSION

A number of newly designed isatin analogs 1-100 were docked into the active sites of different proteins viz., 1RT2, 2VF5, 1EA1 and chimeric 1EA1 respectively by using Glide v 5.0. The binding mode analyses of the compounds with the highest docking scores was carried out and were compared with that of the co-crystallized ligands TNK651, GLP and TPF in the active sites of 1RT2, 2VF5, 1EA1 and chimeric 1EA1, respectively. It was found that compound 47 showed the highest docking score 11.67 in the active site of the NNIBP of RT. However, it was lower than that of the standard TNK 651. It which can be interpreted by the fact that it exhibited two hydrogen bond interactions only in the NNIBP of RT PDB code 1RT2, while compound 88, compound 13, and compound 38 showed highest docking score of −7.31, −7.12 and −8.54 respectively in the active sites of GlcN6P (PDB code 2VF5), MTB-CYP51 (PDB code 1EA1) and *C. albicans* (CACYP51) (PDB code chimeric-1EA1). Though compound 88 exhibited only four hydrogen bond interactions where as the standard GLP exhibited seven H bond interactions the dock score (−7.31) of compound 88 was higher than that of the reference standard GLP (−6.56). However, compound 13 in the active site of 1EA1 showed only one hydrogen bond interaction with a dock score (−7.12), which was higher than that of the reference standard CYP51 (−5.735). Similarly, compound 38 also showed one hydrogen bond interaction, though the dock score (−8.54) was much higher than that of the reference standard CACYP51 (−5.735). The high docking score may be attributed to the favorable interactions of the compound in the active site of chimeric 1EA1 as detailed above. In all cases, the isatin moiety was oriented in a similar way as the reference ligand in the active sites of proteins 1RT2, 2VF5, 1EA1and chimeric 1EA1 respectively. Thus, these studies indicate that the newly designed isatin analogs may have a good binding affinity for enzymes namely HIV-1 RT, GlcN6P, MT-CYP51) and *C. albicans* (CACYP51). ADME properties of all the newly designed compounds was studied by QikProp v3.0. All the designed compounds were found to exhibit lead like properties from the calculated ADME properties. It can be concluded that the isatin moiety flanked by aryl rings substituted particularly with methyl, methoxy and chloro groups with a CH_2CONH linker at the first position of the isatin ring structure may serve as a prominent scaffold for the design and development of HIV-1-RT inhibitors with broad-spectrum chemotherapeutic properties.

ACKNOWLEDGMENTS

The authors are grateful to Birla Institute of Technology for providing the necessary infrastructural facilities and one of the authors BD gratefully acknowledges the University Grants Commission-Basic Science Research (UGC-BSR) for the award of fellowship during the work.

REFERENCES

1. Catalan J, Collins P, Mash B, Freeman M. Mental Health and HIV/AIDS: Psychotherapeutic Interventions in Antiretroviral (ARV) Therapy for Second Level Care. Johannesburg, South Africa: WHO; 2005.
2. Gonda MA, Braun MJ, Clements JE, Pyper JM, Wong-Staal F, Gallo RC, *et al.* Human T-cell lymphotropic virus type III shares sequence homology with a family of pathogenic lentiviruses. Proc Natl Acad Sci U S A 1986;83(11):4007-11.
3. Gonda MA, Wong-Staal F, Gallo RC, Clements JE, Narayan O, Gilden RV. Sequence homology and morphologic similarity of HTLV-III and visna virus, a pathogenic lentivirus. Science 1985;227(4683):173-7.
4. UNAIDS/WHO. AIDS Epidemic Update, 2007. Available from: http://www.data.unaids.org. [Last accessed on 2014 Mar 12].
5. UNAIDS/WHO. Report on the Global AIDS Epidemic, 2008. Available from: http://www.unaids.org/en/KnowledgeCenter/HIVData/GlobalReport/2008/2008 Global report.asp. [Last accessed on 2014 Mar 12].
6. Ghosh TK. AIDS: A serious challenge to public health. J Indian Med Assoc 1986;84(1):29-30.
7. Zeng M, Paiardini M, Engram JC, Beilman GJ, Chipman JG, Schacker TW, *et al.* Critical role of CD4 T cells in maintaining lymphoid tissue structure for immune cell homeostasis and reconstitution. Blood 2012;120(9):1856-67.
8. Effros RB, Fletcher CV, Gebo K, Halter JB, Hazzard WR, Horne FM, *et al.* Aging and infectious diseases: Workshop on HIV infection and aging: What is known and future research directions. Clin Infect Dis 2008;47(4):542-53.
9. Beale MJ Jr, Block JH. Wilson and Gisvold's Text Book of Organic Medicinal and Pharmaceutical Chemistry. 12th ed. New York: Lippincott William Sons Publishers; 2011. p. 347.
10. Snider DE, Raviglione M, Kochi A. Global burden of tuberculosis. Tuberculosis: Pathogenesis, Protection, and Control. Washington, DC: American Society for Microbiology; 1994. p. 3-11.
11. Dye C, Scheele S, Dolin P, Pathania V, Raviglione MC. Consensus statement. Global burden of tuberculosis: Estimated incidence, prevalence, and mortality by country. WHO Global Surveillance and Monitoring Project. JAMA 1999;282(7):677-86.
12. WHO. Global Tuberculosis Report, 2013. Available from: http://www.who.int/tb/publications/global_report/gtbr13_main_text.pdf. [Last accessed on 2014 Jun 14].
13. Sterling TR, Pham PA, Chaisson RE. HIV infection-related tuberculosis: Clinical manifestations and treatment. Clin Infect Dis 2010;50 Suppl 3:S223-30.
14. Abdool Karim SS, Naidoo K, Grobler A, Padayatchi N, Baxter C, Gray A, *et al.* Timing of initiation of antiretroviral drugs during tuberculosis therapy. N Engl J Med 2010;362(8):697-706.
15. Breen RA, Smith CJ, Bettinson H, Dart S, Bannister B, Johnson MA, *et al.* Paradoxical reactions during tuberculosis treatment in patients with and without HIV co-infection. Thorax 2004;59(8):704-7.
16. WHO. Global Tuberculosis Control: A Short Update to the 2009 Report. Geneva: World Health Organization; 2009. Available from: http://www.whqlibdoc.who.int. [Last accessed on 2014 Jun 12].
17. Elzinga G, Raviglione MC, Maher D. Scale up: Meeting targets in global tuberculosis control. Lancet 2004;363(9411):814-9.
18. Silver LL. Challenges of antibacterial discovery. Clin Microbiol Rev 2011;24(1):71-109.
19. Yu D, Huiyuan G. Synthesis and antibacterial activity of linezolid analogues. Bioorgan Med Chem Lett 2002;12(6):857-9.
20. Koca M, Servi S, Kirilmis C, Ahmedzade M, Kazaz C, Ozbek B, *et al.* Synthesis and antimicrobial activity of some novel derivatives of benzofuran: Part 1. Synthesis and antimicrobial activity of (benzofuran-2-yl) (3-phenyl-3-methylcyclobutyl) ketoxime derivatives. Eur J Med Chem 2005;40(12):1351-8.
21. Rippon JW. Monitored environment system to control cell growth, morphology, and metabolic rate in fungi by oxidation-reduction potentials. Appl Microbiol 1968;16(1):114-21.
22. Lagoja IM, Pannecouque C, Van Aerschot A, Witvrouw M, Debyser Z, Balzarini J, *et al.* N-aminoimidazole derivatives inhibiting retroviral replication via a yet unidentified mode of action. J Med Chem 2003 10;46:1546-53.
23. Ganguly S, Debnath B. Molecular docking studies and adme prediction of novel Isatin analogs with potent anti-EGFR activity. Med Chem 2014;4:558-68.
24. Pandeya SN, Sriram D, Nath G, De Clercq E. Synthesis antibacterial, antifungal and anti HIV activity of Schiff"s and Mannich bases of isatin with N-[6-chlorobenz thiazole-2-yl] thiosemicarbazide. Indian J Pharm Sci 1999;61:358-61.
25. Pandeya SN, Sriram D, Nath G, De Clercq E. Synthesis, antibacterial, antifungal and anti-HIV activities of norfloxacin mannich bases. Eur J Med Chem 2000;35(2):249-55.
26. Sarangapani MR, Reddy VM. Pharmacological evaluation of 1-(N,N-disubstituted aminomethyl)-3-imino-(2-phenyl-3,4-dihydro-4-oxo-quinazolin-3-yl) indolin-2-ones. Indian J Pharm Sci 1994;56:174-7.
27. Varma RS, Nobles WL. Antiviral, antibacterial, and antifungal activities of isatin N-Mannich bases. J Pharm Sci 1975;64(5):881-2.
28. Sridhar SK, Saravanan M, Ramesh A. Synthesis and antibacterial screening of hydrazones, Schiff and Mannich bases of isatin derivatives. Eur J Med Chem 2001;36(7-8):615-25.
29. Logan JC, Fox MP, Morgan JH, Makohon AM, Pfau CJ. Arenavirus inactivation on contact with N-substituted isatin beta-thiosemicarbazones and certain cations. J Gen Virol 1975;28(3):271-83.

30. Varma RS, Nobles WL. Synthesis and antiviral and antibacterial activity of certain N-dialkylaminomethylisatin beta-thiosemicarbazones. J Med Chem 1967;10(5):972-4.
31. Singh SP, Shukla SK, Awasthi LP. Synthesis of some 3-(40-nitrobenzoylhydrazone)-2- indolinones as potential antiviral agents. Curr Sci 1983;52(16):766-9.
32. Pandeya SN, Sriram D, Nath G, De Clercq E. Synthesis, antibacterial, antifungal and anti-HIV evaluation of Schiff and Mannich bases of isatin derivatives with 3-amino-2-methylmercapto quinazolin-4(3H)-one. Pharm Acta Helv 1999;74(1):11-7.
33. Pandeya SN, Yogeeswari P, Sriram D, de Clercq E, Pannecouque C, Witvrouw M. Synthesis and screening for anti-HIV activity of some N-Mannich bases of isatin derivatives. Chemotherapy 1999;45(3):192-6.
34. Khan KM, Khan M, Ali M, Taha M, Rasheed S, Perveen S, *et al.* Synthesis of bis-Schiff bases of isatins and their antiglycation activity. Bioorg Med Chem 2009;17(22):7795-801.
35. Verma M, Pandeya SN, Singh KN, Stables JP. Anticonvulsant activity of Schiff bases of isatin derivatives. Acta Pharm 2004;54:49-56.
36. Smitha S, Pandeya SN, Stables JP, Ganapathy S. Anticonvulsant and sedative-hypnotic activities of N-acetyl/methyl isatin derivatives. Sci Pharm 2008;76:621.
37. Venkateshwarlu E, Rao JV, Umasankar K, Dheeraj G. Study of anti-inflammatory, analgesic and antipyretic activity of novel isatin derivatives. Asian J Pharm Clin Res 2012;5(4):187-90.
38. Chandra PM, Venkateshwar J. Biological evaluation of Schiff bases of new isatin derivatives for anti Alzheimer's activity. Asian J Pharm Clin Res 2014;7(2):114-7.
39. Bhattacharya SK, Chakrabarti A. Dose-related proconvulsant and anticonvulsant activity of isatin, a putative biological factor, in rats. Indian J Exp Biol 1998;36(1):118-21.
40. Matesic L, Locke JM, Bremner JB, Pyne SG, Skropeta D, Ranson M, *et al.* N-phenethyl and N-naphthylmethyl isatins and analogues as *in vitro* cytotoxic agents. Bioorg Med Chem 2008 15;16:3118-24.
41. Hossain MM, Islam N, Khan R, Islam M. Cytotoxicity study of dimethylisatin and its heterocyclic derivatives. Bangladesh J Pharmacol 2008;2:66-70.
42. Vine KL, Locke JM, Ranson M, Pyne SG, Bremner JB. *In vitro* cytotoxicity evaluation of some substituted Isatin derivatives. Bioorgan Med Chem 2007;15:931-8.
43. Pervez H, Ramzan M, Yaqub M, Mohammed Khan K. Synthesis, cytotoxic and phytotoxic effects of some new N4-aryl substituted isatin-3-thiosemicarbazones. Lett Drug Des Discov 2011;8:452-8.
44. Shuttleworth SJ, Nasturica D, Gervais C, Siddiqui MA, Rando RF, Lee N. Parallel synthesis of isatin-based serine protease inhibitors. Bioorg Med Chem Lett 2000;10(22):2501-4.
45. Jones G, Willett P. Docking small-molecule ligands into active sites. Curr Opin Biotechnol 1995;6:652-6.
46. Muegge I, Rarey M. Small molecule docking and scoring. Rev Comput Chem 2001;17:1-60.
47. Krovat EM, Steindl T, Langer T. Recent advances in docking and scoring. Curr Comput Aided Drug Des 2005;1:93-102.
48. Friesner RA, Banks JL, Murphy RB, Halgren TA, Klicic JJ, Mainz DT, *et al*. Glide: A new approach for rapid, accurate docking and scoring. Method and assessment of docking accuracy. J Med Chem 2004;47:1739-49.
49. Available from: http://www.rcsb.org/pdb. [Last accessed on 2014 Mar 14].
50. Vijesh AM, Isloor A, Telkar S, Arulmoli T. Molecular docking studies of some new imidazole derivatives for antimicrobial properties. Arab J Chem 2013;6(2):197-204.
51. Yoshida Y, Aoyama Y. Yeast cytochrome P-450 catalyzing lanosterol 14 alpha-demethylation. I. Purification and spectral properties. J Biol Chem 1984;259(3):1655-60.
52. Hitchcock CA, Dickinson K, Brown SB, Evans EG, Adams DJ. Purification and properties of cytochrome P-450-dependent 14 alpha-sterol demethylase from *Candida albicans*. Biochem J 1989;263(2):573-9.
53. Rossello A, Bertini S, Lapucci A, Macchia M, Martinelli A, Rapposelli S, *et al.* Synthesis, antifungal activity, and molecular modeling studies of new inverted oxime ethers of oxiconazole. J Med Chem 2002;45(22):4903-12.
54. Carlson HA, Masukawa KM, McCammon JA. Method for including the dynamic fluctuations of a protein in computer-aided drug design. J Phys Chem 1999;103:10213-9.
55. Carlson HA, Masukawa KM, Rubins K, Bushman FD, Jorgensen WL, Lins RD, *et al.* Developing a dynamic pharmacophore model for HIV-1integrase. J Med Chem 2000;43(11):2100-14.
56. Schrodinger, LLC. New York, USA: Schrodinger Inc.; 2008.
57. Lipinski CA, Lombardo F, Dominy BW, Feeney PJ. Experimental and computational approaches to estimate solubility and permeability in drug discovery and development settings. Adv Drug Deliv Rev 2012;64:4-17.